ELSEVIER

International Journal of Inorganic Materials 3 (2001) 51–58

International Journal of Inorganic Materials

Effect of doping elements on the thermal stability of transition alumina

Sylvie Rossignol*, Charles Kappenstein

Laboratoire de Catalyse en Chimie Organique, UMR 6503, Faculté des Sciences, 40 Avenue du Recteur Pineau, 86022 Poitiers, France

Accepted 21 June 2000

Abstract

The thermal stability of porous transition alumina at high temperature is a crucial challenge for several applications. To delay the θ to α-alumina transition temperature (1180°C), the synthesis by sol–gel method and the introduction of doping element as nitrate salt $M(NO_3)_x$ (M=Ba, Mg, Pr, La and Ce) have been investigated. Over three preparation procedures, the introduction of the doping element through the sol–gel process gave the higher BET surface area. Additional thermal analysis and powder X-ray diffraction studies have shown that only a few amount (1 mol percent) of doping element is sufficient to increase the θ→α-Al_2O_3 phase transition temperature up to 1315°C. The most promising samples are $(Al_2O_3)_{0.98}Ba_{0.02}$ and $(Al_2O_3)_{0.99}Pr_{0.01}$. Even after 5 h at 1200°C, they maintain a rather good specific area (32 m^2/g) in relation with the incomplete and very slow transformation of θ into α-alumina.

Keywords: Alumina; Thermal stability; Sol gel process; Doping elements

1. Introduction

Many industrial solid catalysts are made up of active centers anchored on transition alumina supports. This is a consequence of the prominent characteristics of such transition aluminas like high porosity and surface area, good mechanical strength and thermal stability. Most of the catalytic processes require only moderate temperature conditions, i.e., much less than 800–900°C, and the thermal stability of the alumina based catalysts remains usually good, even during extended time at temperature.

Other catalytic reactions have been developed which require higher temperatures of the order 1000–1400°C and therefore more stable catalysts. Among these reactions we can cite: catalytic conversion of automotive emission gas [1], high temperature catalytic fuel combustion [2,3], methane steam reforming [4] or catalytic decomposition of monopropellant for space applications [5]. The last application concern the control of position and orientation of satellites which is achieved by using several small thrusters powered by the decomposition of hydrazine flowing on alumina supported iridium catalysts. The use of new monopropellant formulations [6] can increase the impulse of the thrusters and diminish the propellant consumption by rising the temperature of the exhaust gas up to 1500°C.

The necessity to work in high temperature conditions requires the prevention or damaging of the catalysts by improving the high temperature stability of the transition alumina phase which is used as a high surface area support. The thermal stability as well as the mechanical properties of the support thus remain key points, and the surface area of the carrier must stay as high as possible when the reaction temperature increases, in order to avoid loss of active centers.

Therefore the stabilization of transition aluminas is a challenge also relevant to other applications such as the ceramics membranes or the support used for the catalytic conversion of automotive exhaust gas [7–9]. The thermal stability depends on two main ways:

(i) The loss of surface area during the textural transformation of the transition alumina. This transformation involves condensation between hydroxyls on adjacent alumina particles and explain the major influence of water partial pressure [10].

(ii) The structural transformation of transition alumina into well crystallized α-alumina which occurs at around 1200°C and is described by a nucleation and growth

*Corresponding author. Fax: +33-54-945-4020.

E-mail address: sylvie.rossignol@univ-poitiers.fr (S. Rossignol).

1466-6049/01/$ – see front matter
PII: S1466-6049(00)00088-X

mechanism. The rate limiting step is the nucleation of α-Al_2O_3 and the contacts between the alumina particles dominate the sintering process [11].

To prevent or delay the alumina transformations the addition of doping elements has been extensively used [12–16]. Among these the most frequently cited are the lanthanide elements (more often lanthanum) and the alkaline earth metal beside zirconium oxide and silica.

Three main parameters can be distinguished. The first one is the origin of the alumina (industrial or prepared) and the procedure used for its preparation like aqueous precipitation, high temperature ceramics, or sol gel techniques, which leads to interesting results in the case of fume pyrolysis of boehmite sols [17] or drying in supercritical conditions [18]. The second parameter is the nature of the additive and the major characteristic to explain the stabilizing effect is the ionic radius of the added cation [19]. The third parameter concerns the introduction procedure of the doping element such as alkaline earth cations, which appears promising [8,20]: (i) procedure relevant to ceramics, i.e. solid mixture of alumina and oxide of the doping element; (ii) aqueous impregnation of the support (most of the published data); (iii) use of sol gel technique with alcoholate precursors in order to obtain the best interaction between support and additives.

The aim of the present work was to shift the phase transition of alumina towards higher temperatures and to follow the evolution of the surface area and the structure of sol gel alumina doped by alkaline earths or lanthanides. The sol–gel method takes advantages of good reproducibility, one step synthesis of metastable phase and the possibility to introduce the doping element at different stages of the preparation procedure: before the gelation step or after the drying or the calcination steps [21].

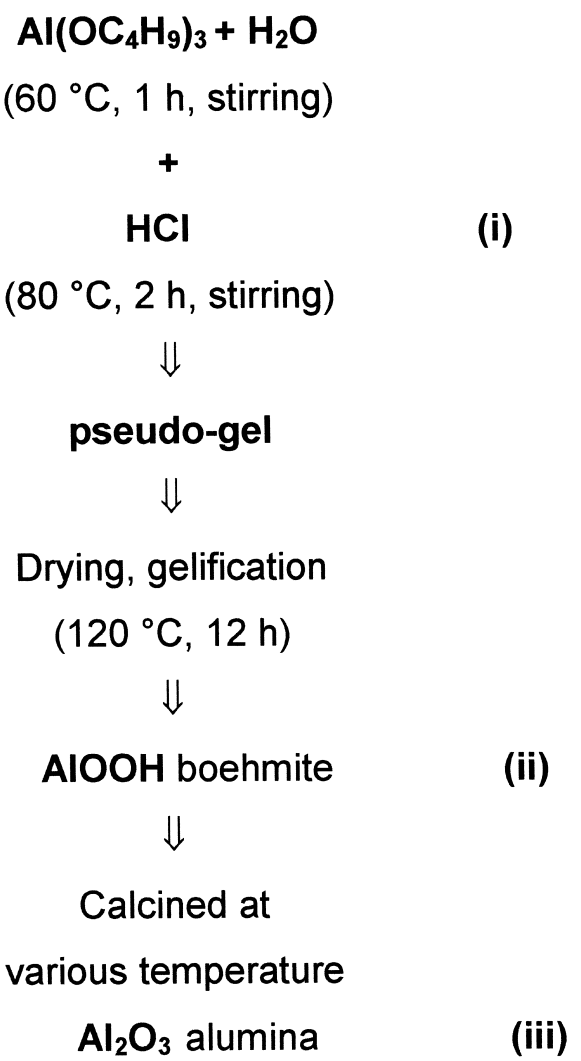

Scheme 1. Description of the preparation procedure for the different samples.

2. Experimental

2.1. Preparation

The procedure described by Yoldas was followed for the synthesis of hydrated boehmite [22]: hydrolysis and peptization of 0.1 mol (25 g) of aluminum trisecbutoxide $Al(OC_4H_9)_3$ with 10 mol water (180 ml) at 60°C under stirring (1 h), followed by addition of 0.01 mol HCl (0.8 ml of 12 mol l^{-1} aqueous solution); then the temperature was raised to 80°C during 2 h (Scheme 1). The xerogel was obtained as hydrated pseudo-boehmite $AlO(OH)\cdot 0.8H_2O$ (S_{BET}=300 m^2 g^{-1}) after drying overnight at 120°C in a ventilated oven. The doping element can be introduce through three methods: (i) during the sol–gel transformation, (ii) by impregnation of the pseudo-boehmite and (iii) by impregnation of alumina obtained by calcination of boehmite at 900°C (S_{BET}=120 m^2 g^{-1}).

For the method (i), the doping element was added as nitrate salt (10 ml of aqueous solution of given concentration) simultaneously with hydrochloric acid. The same conditions were strictly applied for the different sol gel preparations but the kinetic of the sol gel reaction and the intermediate steps were not followed.

For the methods (ii) and (iii), the element was introduced as nitrate salt using the impregnation procedure: an aqueous solution of the doping element (in 10 ml water) was added to a given amount of AlOOH or Al_2O_3 (typically 3 g) and the suspension was stirred at room temperature during (10 min). Then, for each method, the solution was dried in an oven at 120°C during 48 h and further calcined at different temperature (900, 1050, 1200 and 1400°C, heating rate 5°C min^{-1}) in air during 5 h.

The content of doping element ranged from 1 to 14 mol%, depending on the nature of the element. The formula used for the different samples is expressed in molar percent of alumina and atom percent of doping element: $(Al_2O_3)_{(1-x)}M_x$ where M represents the cationic doping element: Ba, Mg, Pr, La and Ce (see Table 1). This

Table 1
Label and composition of samples prepared by sol–gel method

Doping element	Composition (mole)	Composition (weight percent)	Label
–	Al_2O_3	Al_2O_3	(a)
Mg	$(Al_2O_3)_{0.95}Mg_{0.05}$	1.0% Mg	(b)
Ce	$(Al_2O_3)_{0.99}Ce_{0.01}$	1.4% Ce	(c)
Ba	$(Al_2O_3)_{0.98}Ba_{0.02}$	2.7% Ba	(d)
La	$(Al_2O_3)_{0.99}La_{0.01}$	1.4% La	(e)
Pr	$(Al_2O_3)_{0.99}La_{0.01}$	1.4% Pr	(f)

notation does not represent the real composition of the sample, but it is in agreement with the fact that the doping element is generally not present in a separate phase.

All the reagents and solvents were Aldrich products, 99.9% purity. They were used without any further purification: $Ce(NO_3)_3{\cdot}6H_2O$; $Pr(NO_3)_3{\cdot}6H_2O$; $Ba(NO_3)_2$; $La(NO_3)_3{\cdot}6H_2O$; $Mg(NO_3)_3{\cdot}6H_2O$.

2.2. Characterization

Differential thermal analysis (DTA) and thermogravimetric analysis (TGA) were recorded in order to characterize the solids after drying at 120°C. TDA–TGA experiments were carried out between 25 and 1350°C using a Thermal Analyst 2100 TA Instruments. The samples were heated in dry air flow (Air Liquide, France, total impurities <5 ppm; 100 $cm^3\ min^{-1}$) at 10°C min^{-1} for TDA and 1°C min^{-1} for TGA measurements.

Specific surface areas were determined by N_2 adsorption at −196°C (Air Liquide, 30% in He) with a Micromeritics Flow Sorb II apparatus (one point BET method).

XRD analysis of the different powders calcined at various temperatures were carried out by means of a Siemens D5005 powder θ–θ diffractometer using the CuKα radiation (Kα1 = 0.15406 nm) and a graphite back monochromator. The diffractograms were obtained under the following conditions: dwell time: 1 s; step: 0.05°; 2θ range: 10–90°; divergence slit: 1°. Crystalline phases were identified by comparison with PDF standards (Powder Diffraction Files from ICDD).

3. Results and discussion

3.1. Influence of the loading procedure of the doping element

The introduction procedure was studied using two doping elements, magnesium and cerium. Fig. 1 represents the specific area for both doped alumina ($(Al_2O_3)_{0.95}Mg_{0.05}$ and $(Al_2O_3)_{0.99}Ce_{0.01}$) after calcination at 900°C, as well as for pure Al_2O_3 (900°C; sol–gel process) [23]. All samples exhibit the same δ-Al_2O_3 structure (X-rays diffraction, not given), showing no direct influence of the doping element on the structure of these materials. Nevertheless the mode of addition of the additive element displays an obvious influence on the specific area.

For the impregnation procedure on the alumina previously calcined at 900°C, we can observe a slight decrease of the specific area value for both additives. This decrease can be simply explained by a partial blockage of the pores by the foreign ions. On the other hand the impregnation on the high surface area boehmite leads to different results for both cations: area decrease for magnesium and slight increase for cerium, by comparison with undoped alumina.

The samples obtained by the sol–gel method show clearly an increase of surface area: $(Al_2O_3)_{0.95}Mg_{0.05}$ and

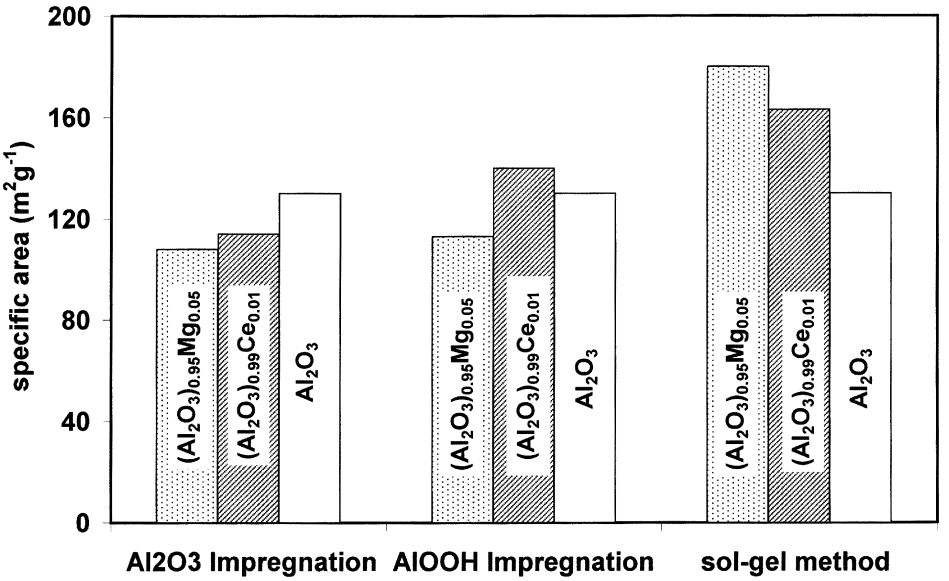

Fig. 1. Influence of the preparation procedure on the specific surface area for undoped and Mg or Ce doped alumina.

$(Al_2O_3)_{0.99}Ce_{0.01}$ display respectively 180 and 163 $m^2\ g^{-1}$ as compared with pure Al_2O_3 sample (130 $m^2\ g^{-1}$). For this temperature range, the loss of specific area is mainly due to the elimination of water from surface hydroxyl groups residing on adjacent particles; this will result in new Al–O–Al bonds with a decrease of the specific surface area. This process can be delayed by the presence of multivalent cations which are located at the surface of the alumina particles and inhibit the binding between particles [24]. The variations of surface area can be therefore be explained by better interactions between additional element and carrier due to the sol gel process, leading to a more homogeneously dispersed additive and a decrease of the surface strain.

Levy and Bauer [25] have shown that the addition of magnesium to industrial alumina through the wetness impregnation procedure leads to a beneficial effect on the surface area after calcination at 600°C and this effect was confirmed by Shaper and Van Reijen [26], Zhu et al. [27] and Ismagilov et al. [16]; these results are in disagreement with the lowering of the surface area for both impregnation procedures and this discrepancy could be explained by the different aluminas used: industrial or sol gel based alumina. The role of cerium is more limited after the impregnation procedure on boehmite, in agreement with the limited interaction between cerium and alumina surface proposed by Koryabkina et al. [28].

Taking into account these results, the next samples were prepared only by means of the sol gel procedure to introduce the doping element.

3.2. Influence of the nature and content of the doping element

The specific area of the different samples after calcination at 900°C, are shown in Fig. 2 as a function of the nature and content of the doping element (Mg, Ba, La or Ce). If we compare the doped aluminas and the pure alumina (doted line), only one sample, containing lanthanum, displays a lower area. For the other samples, a few amount of additives is sufficient to produce an increase of the specific area. The introduction of alkaline earth's (Mg, Ba) in alumina produced a better specific area than the samples doped with the lanthanide elements (Ce, La); therefore the following order can be proposed: Mg≈Ba> Ce>La and this sequence cannot be rationalized on the basis of ionic radius or electrostatic field.

For higher load, a decrease of the specific area is evidenced for all four doping elements and may be explained by a blockage of the smallest pores or by the formation of crystallized mixed oxide phases, which could induce a weak sintering of the support. For the sample doped by magnesium, a maximum is reached at about 4%, in agreement with the results of Levy and Bauer [25] and this can be the consequence of two counterbalanced effects: a better interaction with alumina for low loaded samples and the possible formation of spinel $MgAl_2O_4$ for samples with increased content of magnesium.

3.3. Thermal analysis of sol–gel doped alumina

This part concerns samples containing 1–4 mol% of additive element introduced by sol–gel method; the labels of these solids are gathered in Table 1. Praseodymium was added to the previous additives as it is the next lanthanide element after cerium, displays the same +III most stable oxidation state as La but with a lower ionic radius (0.099 nm for Pr^{3+}; 0.103 nm for La^{3+}); this will allow a comparison between both lanthanides and the effect of ionic radius.

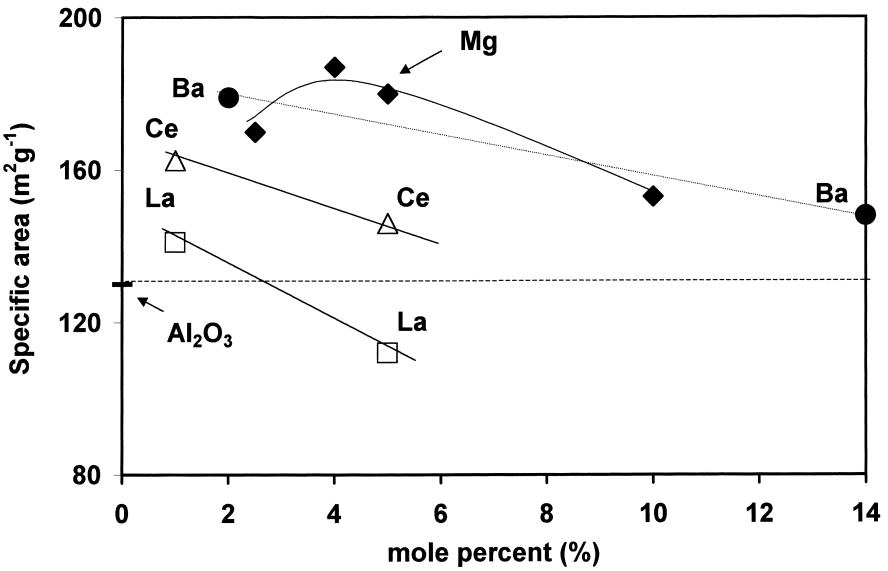

Fig. 2. Influence of the nature and content of doping element on the specific surface for samples prepared via the sol–gel procedure.

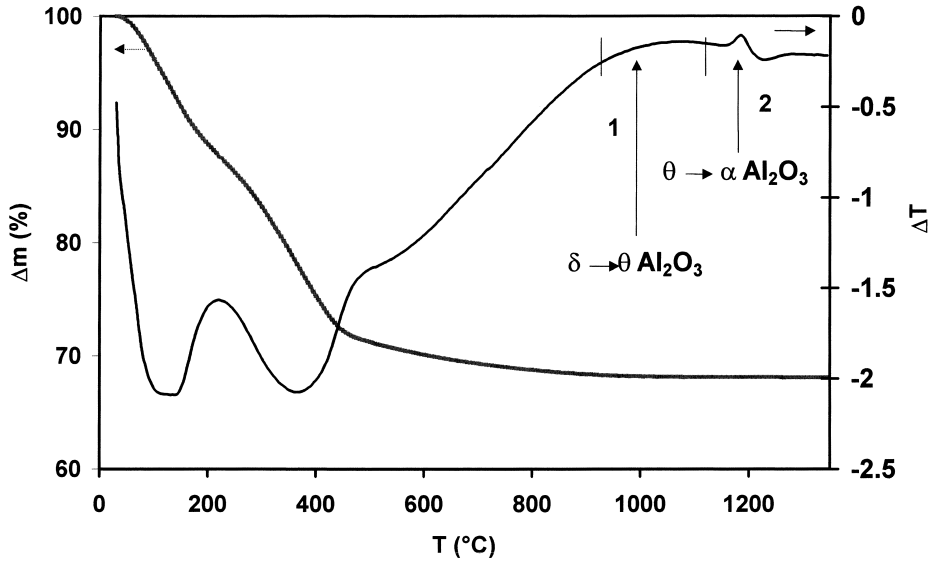

Fig. 3. Thermal analysis (DTA and DGA curves) of the sol–gel sample (b) $Al_2O_{0.96}Mg_{0.04}$.

Fig. 3 shows representative DTA and DGA curves for the dried $(Al_2O_3)_{0.95}Mg_{0.05}$ sample. The profile of the thermogram is in agreement with the results obtained for pure AlOOH boehmite [23]. The two endothermic peaks, respectively at 135 and 375°C, are associated with large weight losses on TGA curve; they are due respectively to the departure of physisorbed water and traces of C_4H_9OH alcohol (boiling point 100°C) from remaining alcoxy groups, for the first wave and then to the decomposition of boehmite AlO(OH) into γ-alumina for the second wave. The two exothermic features 1 and 2, observed at higher temperature, correspond to the formation of better crystallized phases of alumina. The very broad peak centered at about 1000°C and corresponding to the thermal event 1, may be attributed to the $\delta \rightarrow \theta$-$Al_2O_3$ transformation whereas the well defined peak 2 at 1180°C is characteristic of the $\theta \rightarrow \alpha$-$Al_2O_3$ phase transition.

For all samples, similar curves have been obtained into the range 25–900°C, and DTA curves are presented in Fig. 4 for the different samples, only in the range 900–1350°C. Pure alumina carrier (a) and alumina doped with Mg (b), display the same transition temperatures whereas for the other samples, differences can be evidenced. For Ce-doped sample (c), the curve displays three exothermic peaks: the first one is due to the $\delta \rightarrow \theta$-$Al_2O_3$ transition at about 1050°C, the second one at 1200°C may be assigned to the formation of CeO_2, and the third thermal event, which occurs at about 1275°C, is characteristic of the $\theta \rightarrow \alpha$-$Al_2O_3$ transition. The samples doped with Ba (d), La (e) and Pr (f) present the same behavior, with two exothermic peaks corresponding to the $\delta \rightarrow \theta$ and $\theta \rightarrow \alpha$ phase transitions of alumina. Nevertheless, we can note that the last transformation is shifted to higher temperature (1315°C) for the samples (d) and (f) whereas for the La doped sample (e), these transitions occur at lower temperatures.

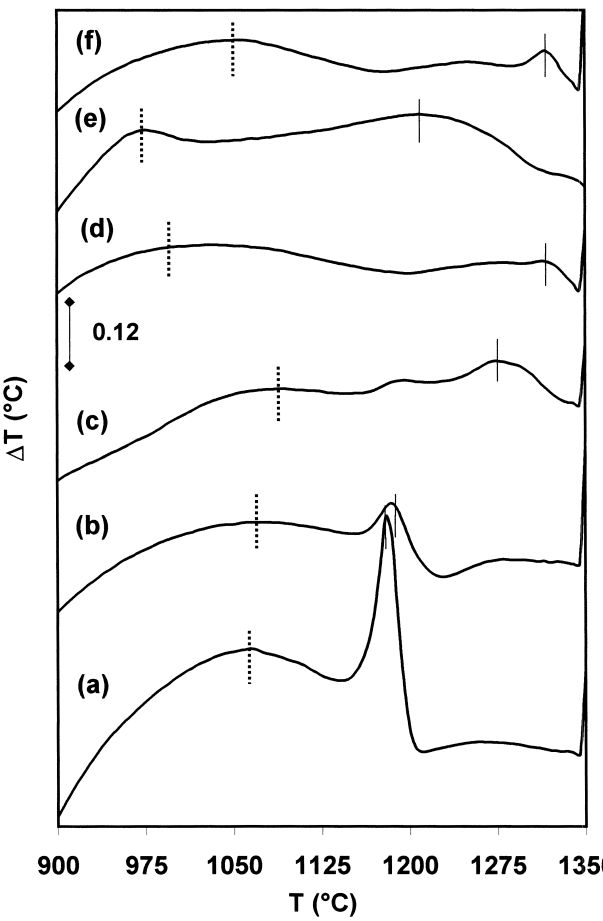

Fig. 4. Enlargement of the thermograms between 900 and 1350°C for the $(A1_2O_3)_{(1-x)}M_{(x)}$ samples. All the curves are on the same scale. Pure alumina (a); M = Mg (b); Ce (c); Ba (d); La (e); Pr (f). Exotherm (1): $\delta \rightarrow \theta$ transition; exotherm (2): $\theta \rightarrow \alpha$ transition.

From these results, the doping elements can be classified into two series, one giving limited effects (Mg, Ce) and the other shifting the $\theta \rightarrow \alpha$-$Al_2O_3$ phase transition to higher temperatures (Ba, La, Pr). The maximum shift is obtained for the doping elements barium and praseodymium.

3.4. X-rays diffraction results

The results of X-ray diffraction studies are summarized in Table 2 and the diffractograms obtained at 1200°C are given in Fig. 5. The structural evolution relative to alumina is in agreement with previous work [23]. After the calcination at 900°C, all the samples display the δ-alumina structure. For pure alumina sample (a), a mixture of α-alumina (corundum) and θ-Al_2O_3 is already observed at 1050°C, after 5 h of calcination, whereas the other samples show a mixture of δ and θ alumina. These mixtures convert into corundum structure at 1200°C for pure alumina (a) and for the magnesium doped sample (b). With cerium, traces of θ-alumina are still observed and for the samples (d), (e) and (f), θ-alumina phase remains important beside corundum. The presence of doping element is revealed for Mg and Ce by the formation of $MgAl_2O_4$ and CeO_2 respectively, as it can be seen in Fig. 5. After a calcination at 1400°C during 5 h, all the solids present the predominant corundum phase mixed with minor binary or ternary oxide phases relative to the doping element.

From these structural results, the doped samples may be divided into two series:

(i) A first one for which the introduction of doping element involves no deep transformation until 1200°C (samples (d), (e) and (f)). We observe at 1050°C a mixture of θ + δ transition alumina which transforms always at 1200°C in a mixture of θ + α transition alumina.

(ii) A second one for which the influence of doping element may be observed from 1050°C (samples (b) and (c)) and is clearly evidenced at 1200°C by the presence of oxides $MgAl_2O_4$ or CeO_2 for the samples (b) or (c).

Taking into account all these observations, the doped samples (d), (e) and (f) remain the most promising to display an expected increase of thermal stability.

The values of the specific area for all samples calcined at different temperature are gathered in Fig. 6. A decrease of the area is observed when the temperature increases up to 1050°C; then a dramatic drop is displayed at 1200°C for the samples (a), (b) and (c), whereas the samples (d), (e), (f) keep an acceptable area. The calcination at 1400°C leads to a very low specific area for the whole samples.

If we compare the whole results, only two samples remain stable after 5 h at 1200°C keeping a rather good specific area in relation with the incomplete transformation of θ-alumina into corundum: alumina doped with barium or praseodymium. Both samples display the same DTA profile (Fig. 4) and the transition temperature of the phase transformation is delayed up to 1315°C displaying a stability increase of 135°C by comparison with pure alumina.

3.5. Comparison with literature data

Table 3 summarizes the specific area results including data taken from literature, for different doping elements [7–9,29–31]. If we compare the three preparation methods for a same doping element, only the sol–gel and impregnation methods remain competitive. The ceramic method produces mainly well crystallized samples with a low specific area [29]. From the literature, the impregnation mode gives better results than the sol–gel method. This fact may be explained by the use of commercial alumina displaying a higher specific area of 170 $m^2 \cdot g^{-1}$ [29,30]. The results obtained by the sol–gel method give

Table 2
Powder X-rays diffraction results of the $(Al_2O_3)_{(1-x)}M_x$ samples (M = Ba, Mg, Ce, La and Pr) calcined 5 h at 900, 1050, 1200 and 1400°C[a]

Samples	*T* (°C)			
	900°C	1050°C	1200°C	1400°C
Al_2O_3 (a)	δ-Al_2O_3 (Q1)	α-Al_2O_3 (R1) θ-Al_2O_3 (M)	α-Al_2O_3 (R1)	α-Al_2O_3 (R1)
$(Al_2O_3)_{0.96}Mg_{0.04}$ (b)	δ-Al_2O_3 (Q1)	δ-Al_2O_3 (Q1) θ-Al_2O_3 (M) $Mg_{0.13}Al_2O_3$ (Q2)	α-Al_2O_3 (R1) $MgAl_2O_4$ (C1)	α-Al_2O_3 (R1) $MgAl_2O_4$ (C1)
$(Al_2O_3)_{0.99}Ce_{0.01}$ (c)	δ-Al_2O_3 (Q1)	δ-Al_2O_3 (Q1) θ-Al_2O_3 (M)	α-Al_2O_3 (R1) θ-Al_2O_3 (M) CeO_2 (C2)	α-Al_2O_3 (R1) CeO_2 (C2)
$(Al_2O_3)_{0.98}Ba_{0.02}$ (d)	δ-Al_2O_3 (Q1)	δ-Al_2O_3 (Q1) θ-Al_2O_3 (M)	α-Al_2O_3 (R1) θ-Al_2O_3 (M)	α-Al_2O_3 (R1) $BaO \cdot 6.6Al_2O_3$ (H1)
$(Al_2O_3)_{0.99}La_{0.01}$ (e)	δ-Al_2O_3 (Q1)	δ-Al_2O_3 (Q1) θ-Al_2O_3 (M)	α-Al_2O_3 (R1) θ-Al_2O_3 (M)	α-Al_2O_3 (R1) $LaAl_{11}O_{18}$ (H2)
$(Al_2O_3)_{0.99}Pr_{0.01}$ (f)	δ-Al_2O_3 (Q1)	δ-Al_2O_3 (Q1) θ-Al_2O_3 (M)	α-Al_2O_3 (R1) θ-Al_2O_3 (M)	α-Al_2O_3 (R1) $PrAlO_3$ (R2)

[a] ICCD Files (Q1, Q2: Quadratic 46-1131, 20-660; R1, R2: Rhomboidal 43-1484, 29-0076; C1, C2: Cubic 47-0254, 43-1002; M: Monoclinic 35-121; H1, H2: Hexagonal 33-128, 33-699).

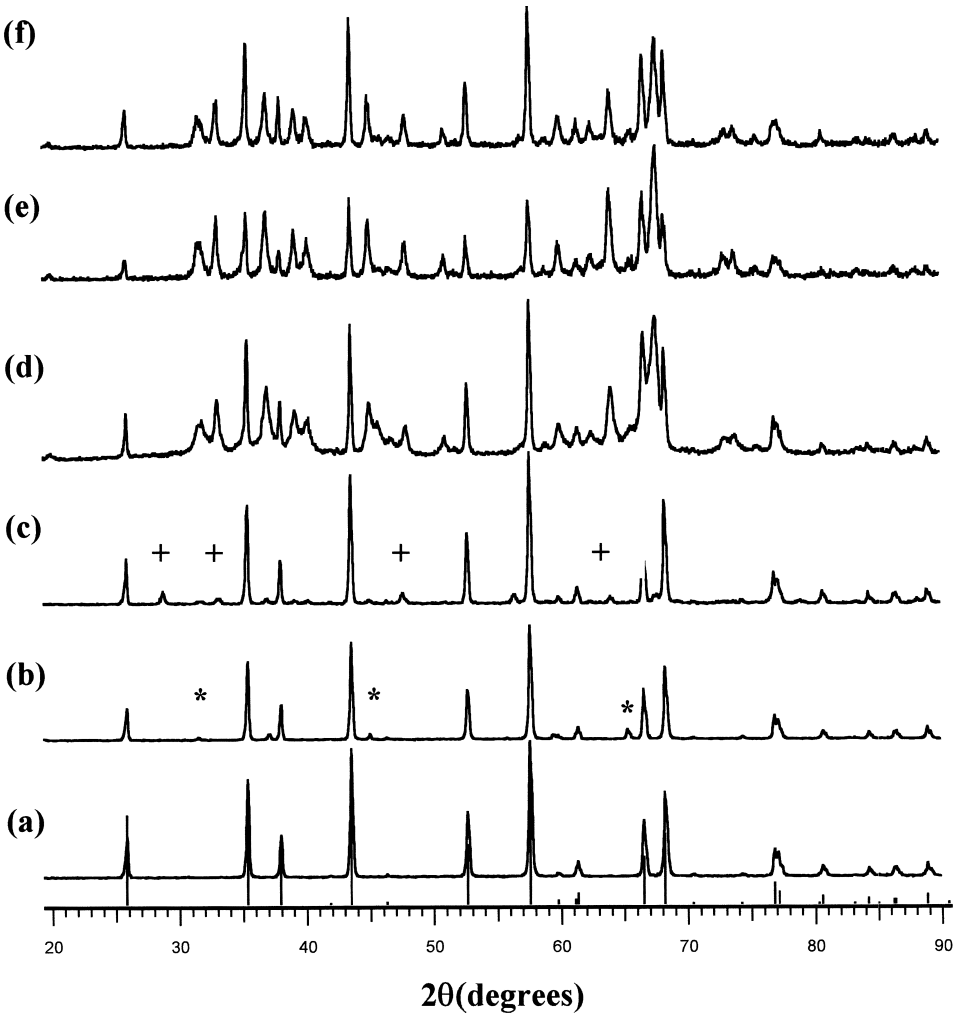

Fig. 5. Diffractograms of the $(A1_2O_3)_{(1-x)}M_{(x)}$ samples calcined at 1200°C. (*: $MgAl_2O_4$; +: CeO_2). The vertical lines on the *x* scale correspond to α-alumina. Pure alumina (a); M=Mg (b); Ce (c); Ba (d); La (e); Pr (f).

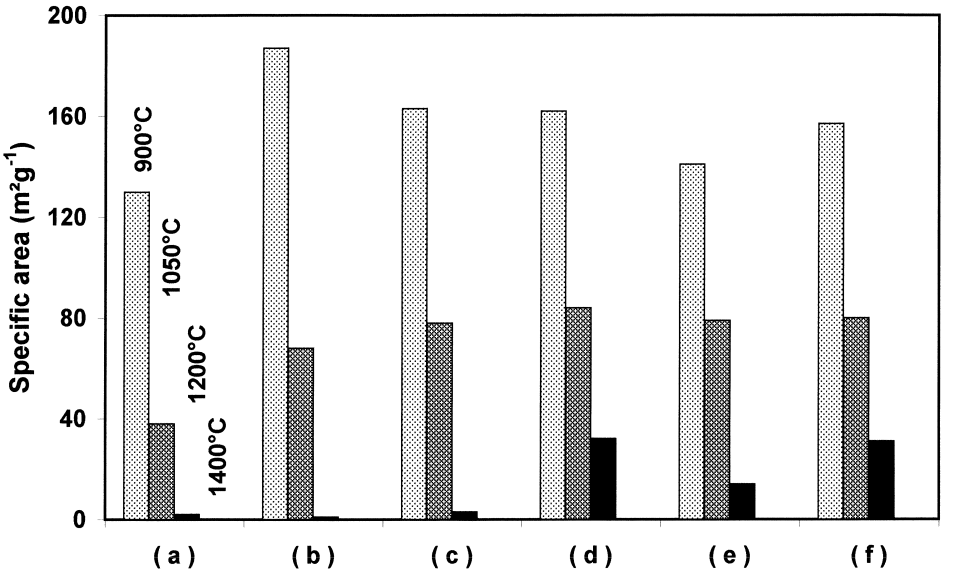

Fig. 6. Specific area of the $(A1_2O_3)_{(1-x)}M_{(x)}$ samples calcined at 900, 1050, 1200 and 1400°C. Pure alumina (a); M=Mg (b); Ce (C); Ba (d); La (e); Pr (f).

Table 3
Comparison with literature data concerning the preparation mode and the doping element of alumina

Preparation mode	Doping element	Atom percent	Specific area $m^2 \cdot g^{-1}$ at 1200°C	References
Ceramic	Ba	0.14	25	[29]
Impregnation	Ce	0.01	40	[8,30,31]
	La	0.01	55	[8,30]
	Gd	0.01	55	[8,30]
Sol–gel	Ba	0.02	41	[7]
	Ba	0.14	50	[29]
	La	0.03	16	[7,20]
Sol–gel	La	0.01	14	This work
	Pr	0.01	31	
	Ce	0.01	3	
	Ba	0.02	32	
	Mg	0.04	1	

similar specific area, and whoever the authors, it appears that:

- The cations Mg^{2+} and Ce^{4+} are not favorable to stabilize the alumina support, owing to the formation of specific phases.
- Among the alkaline earth, the addition of barium is much more beneficial by comparison with magnesium, in relation with the greater ionic radius.
- The dispersion of the results concerning Ba doped alumina can be related to different drying conditions and metal loads.

Praseodymium was less frequently used for this purpose than lanthanum in order to increase the transition temperature of alumina [32–34]. This element seems to be very promising to these studies particularly if it can be associated to drying procedure using supercritical conditions, as it was published in a recent paper [18] which relates an important increase of the thermal stability of non-doped alumina due to this specific method.

4. Conclusion

The high stability of alumina depends on the mode of preparation and on the doping element. From our results, the best method to introduce the doping element, is the sol–gel procedure, which allows for an increase of the interaction of the additional element with the carrier.

Low contents of doping element are sufficient to enhance the thermal stability of alumina and the best additives are barium or praseodymium cations. The structure of the Ba or Pr doped alumina corresponds to a mixture of $\delta+\theta$ alumina phases below 1200°C; at 1200°C, this mixture transforms into $\theta+\alpha$ alumina. A further calcination at 1400°C leads to a drop of the surface area and to the respective formation of $BaO \cdot 6.6Al_2O_3$ or $PrAlO_3$ mixed oxides. These remarks are in agreement with DTA data which show a shift of the transition temperature to α alumina from 1180 to 1315°C.

Acknowledgements

Thanks are due to E. Chatelier for his technical help in carrying out most of the experiments, which are reported in this paper.

References

[1] Lox ESJ, Engler BH. In: Ertl G, Knözinger H, Weitkamp J, editors, Handbook of heterogeneous catalysis, Germany: Wiley–VCH, 1997, p. 1559.
[2] Trimm DL. Catal Today 1995;26:231.
[3] Arai H, Fukuzawa H. Catal Today 1995;26:217.
[4] Kochloefl K. In: Ertl G, Knözinger H, Weitkamp J, editors, Handbook of heterogeneous catalysis, Weinheim, Germany: Wiley–VCH, 1997, p. 1819.
[5] Schmidt E. Hydrazine and its derivatives. preparation, properties, applications, New York: J. Wiley, 1984.
[6] Meinhardt D, Brewster G, Christofferson S, Wucherer EJ. 34th AIAA Joint Propulsion Conference, Cleveland OH, July 1998, Paper 98-4006.
[7] Chai M, Machida M, Eguchi K, Arai H. J Memb Sci 1994;96:205.
[8] Ozawa M, Kimura M, Isogai A. J Less Com Met 1990;162:297.
[9] Long CK, Richardson Jr JW, Osawa M. J Alloys Comp 1997;250:356.
[10] Johnson MFL. J Catal 1990;123:245.
[11] Tijburg IIM, De Bruin H, Elberse PA, Geus JW. J Mater Sci 1991;26:5945.
[12] Burtin P, Brunelle JP, Pijolat M, Soustelle M. Appl Catal 1987;34:225.
[13] Burtin P, Brunelle JP, Pijolat M, Soustelle M. Appl Catal 1987;34:239.
[14] Lafarga D, Lafuente A, Menendez M, Santamaria J. J Membr Sci 1998;147:173.
[15] Kobayashi H, Tadanaga K, Minami T. J Mater Chem 1998;8:1241.
[16] Ismagilov ZR, Shkrabina RA, Koryabkina NA. Catal Today 1999;47:51.
[17] Ishkawa T, Ohashi R, Nakabayashi H, Karuta N, Ueno A, Furuta A. J Catal 1992;134:87.
[18] Pierre AC, Elaloui E, Pajonk GM. Langmuir 1998;14:66.
[19] Church JS, Cant NW, Trimm DL. Appl Catal 1993;101:105.
[20] Lin YS, Vries KJ, Burggraaf AJ. J Mater Sci 1991;26:715.
[21] Livage J. Catal Today 1998;41:3.
[22] Yoldas BE. J Mater Sci 1975;10:1856.
[23] Rossignol S, Nguéfack M, Kappenstein C. To be published.
[24] Johnson MFL. J Catal 1990;123:245.
[25] Levy RM, Bauer DJ. J Catal 1967;9:76.
[26] Shaper H, Van Reijen LL. Mater Sci Monogr 1982;14:173.
[27] Zhu B, Yuan X, Jin S, Lue G, Wu. Shiyou Huagong 1995;24:161 (from abstract).
[28] Koryabkina NA, Shkrabina RA, Ushakov VA, Moroz EM, Lausbeg MF. Ismagilov ZR Kinet Catal 1996;37:117.
[29] Machida M, Eguchi K, Arai K. Bull Chem Soc Jap 1988;61:3659.
[30] Ozawa M, Kimura M. Isogai A J Mater Sci Let 1990;9:709.
[31] Ozawa M, Kimura M. J Mater Sci Let 1990;9:291.
[32] Narula CK, Allard LF, Graham GW. J Mater Chem 1999;9:1155.
[33] Masuda K, Kawai M, Kuno K, Kachi N, Mizukami F. Stud Surf Sci Catal 1991;63:229.
[34] Schwaller JM, Wehrer P, Garin F, Maire G. Ann Chim (Paris) 1989;14:209.